

Novel algorithms for efficiently
accumulating, analysing and
visualising full-waveform LiDAR in
a volumetric representation with
applications to forestry

submitted by

Milto Miltiadou

for the degree of Doctor of Engineering

of the

University of Bath

Centre for Digital Entertainment

and of the

Plymouth Marine Laboratory

NERC Airborne Research Facility

April 2017

COPYRIGHT

Attention is drawn to the fact that copyright of this thesis rests with its author. This copy of the thesis has been supplied on the condition that anyone who consults it is understood to recognise that its copyright rests with its author and that no quotation from the thesis and no information derived from it may be published without the prior written consent of the author.

This thesis may be made available for consultation within the University Library and may be photocopied or lent to other libraries for the purposes of consultation.

Signature of Author.....

Milto Miltiadou

Abstract

no more than 300 words

NOTES:

Blue colour: additions according to Neill's feedback,

Purple colour: addition/corrections according to Mike's comments

Red colour: notes

Gray colour: text that is going to be modified

To be added on top

Abstract

This study focuses on enhancing the visualisations and classifications of forested areas using coincident full-waveform (fw) LiDAR data and hyperspectral images. The ultimate aim is use both datasets to derive information about forests and show the results on a 3D virtual, interactive environment. Influenced by Persson et al (2005), voxelisation is an integral part of this research. The intensity profile of each full-waveform pulse is accumulated into a voxel array, building up a 3D density volume. The correlation between multiple pulses into a voxel representation produces a more accurate representation, which confers greater noise resistance and it further opens up possibilities of vertical interpretation of the data. The 3D density volume is then aligned with the hyperspectral images using a 2D grid similar to Warren et al (2014) and both datasets are used in visualisations and classifications.

Previous work in visualising fw LiDAR has used transparent objects and point clouds, while the output of this system is a coloured 3D-polygon representation, showing well-separated structures such as individual trees and greenhouses. The 3D density volume, generated from the fw LiDAR data, is polygonised using functional representation of object (FReps) and the marching cubes algorithm (Pasko and Savchenko, 1994) (Lorensen and Cline, 1987). Further, an optimisation algorithm is introduced that uses integral volumes (Crow, 1984) to speed up the process of polygonising the volume. This optimisation approach not only works on non-manifold object, but also a speed up of up to 51% was achieved. The polygon representation is also textured by projecting the hyperspectral images into the mesh. In addition, the output is suitable for direct rendering with commodity 3D-accelerated hardware, allowing smooth visualisation.

In future work, the effects of combining both hyperspectral imagery and fw LiDAR in classifications and visualisations are examined. At first, two pixel wise classifiers, a support vector machine and a Bayesian probabilistic model, will be used for testing the effects of the combination in generating tree coverage maps. Higher accuracy classification results are expected when metrics from both datasets are used together. Regarding the visualisations, the differences of applying surface reconstruction versus direct volumetric rendering will be discussed and an ordered tree structure with integral sums of the node values will be used for speeding up the ray-tracing of direct volumetric rendering and improving memory management of aforementioned optimisation algorithm with integral volumes. Further, deferred rendering is suggested for testing the visual human perception of projecting multiple bands of the hyperspectral images on the FW LiDAR

polygon representations. At the end of this project the combination of the datasets will be used along with the watershed algorithm for tree segmentation, which is useful for measuring the stem density of a forest and for tree species classifications.

from EDE:

Firstly, a new and fast way of aligning the FW LiDAR with Remotely Sensed Images has been developed in DASOS and by generating tree coverage maps it was shown that the combination of those datasets confers better remote survey results. This work was presented at the 36th ISRSE International Conference.

Secondly, automated detection of dead trees in native Australian forests has a significant role in protecting animals, which live in those trees and are close to extinction. DASOS allow the generation of 3D signatures characterising dead trees. A comparison between the discrete and FW LiDAR is performed to demonstrate the increased survey accuracy obtained when the FW LiDAR are used.

Finally, the last application is for improving visualisations for foresters. Foresters have a great knowledge about forests and can derive a wealth of information directly from visualisations of the remotely sensed data. This reduces the travelling time and cost of getting into the forests. This research optimises visualisations by using the new FW LiDAR representations and a speed of up to 51% has been achieved.

FW LiDAR has great potentials in forestry and this research has already started to have an impact in the FW LiDAR community by making those huge datasets easier to handle. DASOS is now used at Interpine Group Ltd, a world leading Forestry Company in New Zealand and it has been tested from a PhD student at Bournemouth University who looks into estimating bird distribution in the New Forest. In the future, it is expected that DASOS will be widely used in remote forest surveys (i.e. estimating the commercial value of a forest and detecting infected trees at early stages for treatment).

Acknowledgements

Above all, I would like to express my great gratitude to my industrial supervisors Dr. Michael Grant who had supported me continuously during my research and gave me the freedom to create a project of my own interest.

Then, I would like to thanks Dr. Matthew Brown, who helped me during my first years of my studies by giving me valuable and informative feedback. He was always there to keep me working on the right track.

Equally important is my current supervisor Dr. Neil D.F. Campbell and he is not to be missed from the acknowledgements.

Furthermore, special thanks are given to Dr. Mark Warren, Dr. Darren Cosker, MSc Susana Gonzalez Aracil and Dr. Ross Hill who occasionally advised me during my studies.

It further worth giving credits to my data providers, the Natural Environment Research Council's Airborne Research Facility (NERC ARF) and Interpine Group Ltd.

Last but not least, I am extremely grateful to my funding organisations, the Centre for Digital Entertainment and Plymouth Marine Laboratory, who supported financially and consequently made this research possible.

Abbreviations and Glossary

AGC	Automatic Gain Controller
ALS	Airborne Laser Scanning
APL	Airborne Processing Library
ARF	Airborne Research Facility
CG	Computer Graphics
CHM	Canopy Height Model
CUDA	parallel computing platform available on nvidia graphic cards
DASOS	(δασος=forest in Greek), the open source software implemented for managing FW LiDAR data
DEM	Digital Elevation Model
DTM	Digital Terrain Model (DTM)
FW	Full-Waveform
GB	Gigabyte
GPU	Graphics Processing Unit
LiDAR	Light Detection And Ranging
MRI	Magnetic Resonance Imaging
NASA	National Aeronautics and Space Administration
NDVI	Normalised Difference Vegetation Index
NERC	Natural Environment Research Council
NIR	Near-Infrared Region of the electromagnetic spectrum
QGIS	Quantum Geographic Information System
SIMD	Single Instruction, Multiple Data
TB	Terabyte
VIS	Visual Spectrum
VLR	Variable Length Records
WPDF	Waveform Packet Descriptor Format
UK	United Kingdom

Publications

DASOS-User Guide, M. Miltiadou, N.D.F Campbell, M. Brown, S.C. Aracil, M.A. Warren, D. Clewley, D.Cosker, and M. Grant, Full-waveform LiDAR workshop at Interpine Group Ltd, Rotorua NZ, 2016

Improving and Optimising Visualisations of full-waveform LiDAR data, M. Miltiadou, M. Brown, N.D.F Campbell, D. Cosker, M. Grant, *EuroGraphics UK, Computer Graphics & Visual Computing*, 2016

University of Bath Alignment of Hyperspectral Imagery and Full-Waveform LiDAR data for visualisation and classification purposes, M. Miltiadou, M. A. Warren, M. Grant, and M. Brown, *The International Archives of Photogrammetry, Remote Sensing and Spatial Information Sciences*, vol. 40, no. 7, p. 1257, 2015.

Reconstruction of a 3D Polygon Representation from Full-Wavefrom LiDAR data, M. Miltiadou, M. Grant, M. Brown, M. Warren, and E. Carolan, *RSPSoc Annual Conference, New Sensors for a Changing World*, 2014.

Awards

EDE and Ravenscroft Prize - Finalist: Selected as one of the five finalists for this is a prestigious prize that recognises the work of best postgraduate researchers.

Student Poster Competition at Silvilaser.

Conference Presentations

Remote Sensing Cyprus (RSCy) Conference, 2017 , Paphos, Cyprus - Oral Presentation

ForestSAT Conference,2016 , Santiago, Chile - Oral Presentation

Computer Graphics & Visual Computing (CGVC),2016, Bournemouth, United Kingdom - Poster Presentation

Silvilaser, 2015, La Grant Motte, France - Oral Presentation

International Symposium of Remote Sensing of the Environment (ISRSE), 2015, Berlin, German - Oral Presentation

Remote Sensing and Photogrammetry Society (RSPSoc) Conference, New Sensors for a Changing world , 2014, Aberystwyth, United Kingdom - Oral Presentation

Workshops

Full day workshop about FW LiDAR and DASOS at *Interpine Ltd Group*, 2016,
Rotorua, New Zealand

Demonstration of DASOS_v2 at the practical LiDAR session at *the NERC ARF annual workshop*, 2017, Plymouth, United Kingdom

Contents

Abstract	i
Acknowledgements	iii
Abbreviations and Glossary	iv
Publications	v
Awards	v
Conference Presentations	v
Workshops	vi
List of Figures	ix
1 Introduction	1
1.1 Forest Monitoring: Importance and Applications	1
1.2 Background Information about Remote Sensing and Airborne Laser Scan- ning Systems	1
2 Acquire Data	2
3 Overview of Thesis	3
4 The open source software DASOS and the Voxelisation Approach	4
5 Surface Reconstruction from Voxelised FW LiDAR Data	5
6 Optimisation Attempts for the Surface Reconstruction	6
7 Alignment with Hyperspectral Imagery	7
8 Detection of Dead Standing Eucalyptus For Managing Biodiversity in Native Australian Forest	8
8.1 Introduction	8
8.2 Materials and Methods	11

8.3 Results	13
8.4 Discussion	13
9 Comparison with Discrete Data	14
10 Overall Results	16
11 Conclusions	17
11.1 Contributions	18
Bibliography	18
A DASOS user guide	i
B Case Study: Field Work in New Forest	ii
B.1 Introduction	ii
B.2 Validation Data Collected	iii
B.3 Landscape types	vii
B.4 Conclusions and Discussion	x

List of Figures

8-1	Animals Closes to Extinction	10
8-2	LiDAR point cloud showing that there are very limited points reflected from tree trunks.	11
8-3	The shape of dead trees significantly varies from the each other. Here there is an example of two dead trees.	12
8-4	Example of a dead tree in relation to the discrete LiDAR point cloud. .	13
B-1	The first area of interest and the related maps.	v
B-2	The second area of interest and the related maps.	vi
B-3	Trees that have been cut down	vii
B-4	Grass with a few scattered trees	vii
B-5	Dense forest	vii
B-6	Trees that have been cut down	viii
B-7	Lakes and rivers	viii
B-8	Trees that have been cut down	ix
B-9	Animals in New Forest	ix
B-10	Trees, which are mixed together	x

Chapter 1

Introduction

- 1.1 Forest Monitoring: Importance and Applications
- 1.2 Background Information about Remote Sensing and Airborne Laser Scanning Systems

Chapter 2

Acquire Data

Chapter 3

Overview of Thesis

Chapter 4

The open source software DASOS and the Voxelisation Approach

Chapter 5

Surface Reconstruction from Voxelised FW LiDAR Data

Chapter 6

Optimisation Attempts for the Surface Reconstruction

Chapter 7

Alignment with Hyperspectral Imagery

Chapter 8

Detection of Dead Standing Eucalyptus For Managing Biodiversity in Native Australian Forest

8.1 Introduction

8.1.1 The Importance of Dead Wood

The value of dead trees from a biodiversity management perspective is large. Once a tree dies, its contribution to our ecosystem continues. The woody structure remains for centuries and it contributes to forest regeneration while providing resources for numerous surrounding organisms [71]. As an indication, more than 4000 species inhabit dead wood in Finland [72], where an estimate of 1000 species has been extinct [73]. These species do not only include animals and birds but also organisms, like fungi. Fungi contributes to wood decaying, formation of hollows and biodiversity, which is an important factor for a resilient ecosystem [74]. Observing the changes of fungal diversity on decaying wood has an increased interest in science [75] [76] [77] in order to ensure the continuous existence of decaying wood in forests.

Specifically in Australia, tree hollows play a significant role in managing biodiversity. Nearly all arboreal mammals rely on hollows with the exception of the Koala and perhaps Ringtail Possums that preferentially make a stick nest, but they use hollows as well. Additionally, a large number of Australian bird species rely on hollows for shelters [5]. Nevertheless, Australia has no real hollow creators like the northern hemisphere

(e.g. Woodpeckers), and therefore it relies predominantly on natural processes of limb breakage, insect and fungal attack when access points are provided through damage caused by wind, storms and fire.

This kind of hollows take hundreds of years to form and because of that it is more likely to exist on dead trees. In Australia, studies predict shortage of hollows for colonisation in the near future [3] [4]. Therefore automated detection of them plays a significant role in protecting those animals. As an indicator of the importance of hollows in managing biodiversity, a list of a few of the species that rely on hollows was provided by the Forestry Corporation of NSW. Those species are shown at Figure 8-1. According to the Department of the Environment of Australian Government and the Government of Western Australia, six of them are protected, threatened or close to extinct [78] [79]. Figure 8-1 shows the species from the provided list and the six protected species have a red border and their names are bold in the description.

For the aforementioned reasons, monitoring dead trees is essential for having a resilient ecosystem. Nevertheless, the distribution of dead trees significantly varies making detection of them difficult [80]. Remote sensing approaches has been introduce to automate the process of monitoring forest and further increase the spatial resolution of the monitored area. The following section gives an overview of the related work undertaken in Remote Sensing.

8.1.2 Related Work

Remote Sensing was introduced for automatically detecting dead trees, because field-work is time consuming considering their variance spread and the size of the relevant forests. From a classification perceptive, the task of identifying dead standing and dead fallen trees is different. Fallen trees are identified by detecting segments or line-like features on the terrain surface using LiDAR data [81] [82]. Regarding standing dead trees, their shape (reduced number of leaves or broken branches) [83] and light reflectance (less green light illuminated) [84] are important factors for identifying them.

Previous work on dead standing trees detection performs single tree crown delineation before health assessment [83] [85]. Tree-crown delineation is usually done by detecting local maxima from the canopy height model (CHM) and then segmenting trees with watershed algorithm [86]. Improvements has been achieved by introducing markers controlled watershed [87] and structural elements of tree crowns with different sizes [88]. Additionally, Popescu and Zhao analyse the vertical distribution of the LiDAR points in conjunction with the local maximum filtering of CHM [89].

In the case of Eucalyptus, single tree detection is a challenge on its own, due to their irregular structure and multiple trunk splits. In other words, each tree trunks splits



Figure 8-1: A number of species that rely on tree hollows of which the red ones / bold ones are close to extinction: Kookaburra, Sulphur Crested Cockatoo, **Corella**, Crimson Rosella, Eastern Rosella, Galah, Rainbow Lorikeet, Musk Lorikeet, Little Lorikeet , Red-winged Parrot, **Superb Parrot**, Cockatiel, Australian Ringneck (Parrot), Red-rumped Parrot, Powerful Owl, Sooty Owl, Barking Owl, **Masked Owl**, **Barn Owl**, White-throated Treecreeper, Hollow Owl, **Brush-tailed Possum** (mammal) ¹

¹The images of the birds were taken from the following links (Retrieved on the 27th of April 2016): Kookaburra: <<http://tenrandomfacts.com/blue-winged-kookaburra/>>, Sulphur Crested Cockatoo: <<http://aussiegal17.deviantart.com/art/Sulphur-Crested-Cockatoo-08-153341893>>, Corella: <<http://www.theparrotplace.co.nz/all-about-parrots/long-billed-corella/>>, Superb Parrot: <<http://www.davidkphotography.com/?showimage=637>>, Crimson Rosella: <http://25.media.tumblr.com/tumblr_m3mo89c40r1r4t9h1o1_1280.jpg>, Eastern Rosella: <http://2.bp.blogspot.com/-pYxw51WjSOY/UB-LEFgd2KI/AAAAAAAAGw/9z60PUWE6TE/s1600/_GJS6601-as-Smart-Object-1.jpg>, Rainbow Lorikeet: <https://www.reddit.com/r/pics/comments/328fvc/a_rainbow_lorikeet_found_in_coastal_regions/>, Musk Lorikeet: <http://www.rymich.com/girraween/photos/animals/birds/medium/glossopsitta_concinna/glossopsitta_concinna_001.jpg>, Little Lorikeet: <<http://www.pbase.com/sjmurray/psittacidae>>, Red-winged Parrot: <<https://www.pinterest.com/pin/395894623469889727/>>, Cockatiel: <<http://up.parsipet.ir/uploads/Cockatiels-for-sale.jpg>>, Australian Ringneck (Parrot): <<http://ontheroadmagazine.com.au/wp-content/uploads/2015/09/Twenty-eight-parrot-2-min.jpg>>, Red-rumped Parrot: <<http://parrotfacts.net/wp-content/uploads/Red-Rumped-Parrot-on-a-tree.jpg>>, Powerful Owl: <http://farm1.staticflickr.com/219/495796536_f78dac04c1.jpg>, Sooty Owl: <http://www.mariewinn.com/marieblog/uploaded_images/screech2-738532.jpg>, Barking Owl: <<http://www.pcpimages.com/Nature-and-Wildlife/Birds/i-7JKSTp5/1/L/owl%20%281%20of%201%29-L.jpg>>, Masked Owl: <http://www.survival.org.au/images/birds/masked_owl_2_600.jpg>, Galah: <<https://www.pinterest.com/pin/537546905498955709/>>, White-throated Treecreeper: <<https://geoffpark.files.wordpress.com/2011/09/female-white-throated-treecreeper.jpg>>,

create a local maximum leading into over-segmentation when tree crowns are detected by local maxima filtering. Shendryk published a eucalyptus delineation algorithm that starts segmentation from bottom to top. In this paper, the trunks point cloud is separated from the leaves and individual trunks are identified before proceeding to crown segmentation [90]. Nevertheless, there is the consideration of optimal resolution for a cost effective versus quality acquisition [91]. For this project, there is an average of four pulses per square meter, which is considered an optimal resolution. But because of the tree height (up to 43meters according to the fieldwork), a small amount of pulse intensity reached the trunks and the recorded waveform do not include enough information for individual trunk detection. An example of this project's discrete LiDAR data is shown in Figure 8-2 and the missing information about the trunks are depicted.

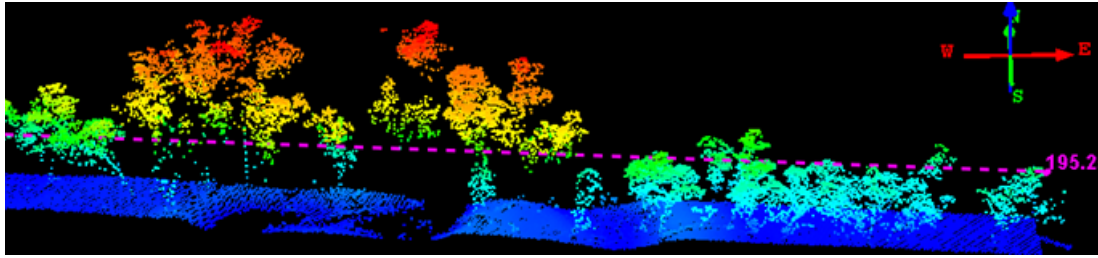


Figure 8-2: LiDAR point cloud showing that there are very limited points reflected from tree trunks.

Here, it is introduced an approach for quick dead tree detection derived from the boost cascade approach [92] but extended into 3D. This approach further contains similarities of the 3D tree shape signatures proposed by Dong, 2009, for distinguishing Oaks from Douglas fir tree crowns [93].

8.2 Materials and Methods

8.2.1 Study Site

8.2.2 Field Data

33 plots allocated randomly in the area of interest Plot Radius: 35.68m GPS tree location Tree information like Dead trees 2386 Trees 269 Dead Trees

8.2.3 Trimble full-waveform LiDAR data

The data, provided by RPS Australia East Pty Ltd, were collected in March 2015 from the Riegl (LMS-Q780 or LMS-Q680i?) sensor at an Australian native Forest

Hollow Owl: <http://www.mariewinn.com/marieblog/uploaded_images/screech2-738532.jpg>



Figure 8-3: The shape of dead trees significantly varies from each other. Here there is an example of two dead trees.

with eucalyptus. The fieldplots have been provided by (Interprine Group Ltd or Forest Corporation?). The LiDAR data used for this project are provided by RPS Australia East Pty Ltd and they were collected in March 2015 using the Riegl (LMS-Q780 or LMS-Q680i?) sensor. The Riegl LMS-Q??? is a native full-waveform sensor and the LiDAR point clouds were generated from the waveform instrument data during post processing. In addition, the field plots used for the classifications are provided by (Interprine Group Ltd or Forest Corporation?) and contain around 1000 Eucalypt trees while 10% of them are dead.

8.2.4 Statistical Analysis

8.2.4.1 The 3D-priors feature of DASOS

The 3D shape signatures were generated by getting the distance distribution of random LiDAR point pairs of the two tree crown classes: Oaks and Douglas [93]

In this chapter, the 3rd feature of DASOS (Table ??) is used for generating 3D priors characterising dead standing Eucalypt trees. These 3D priors are used for detecting dead standing Eucalypt trees in native Australian forests.

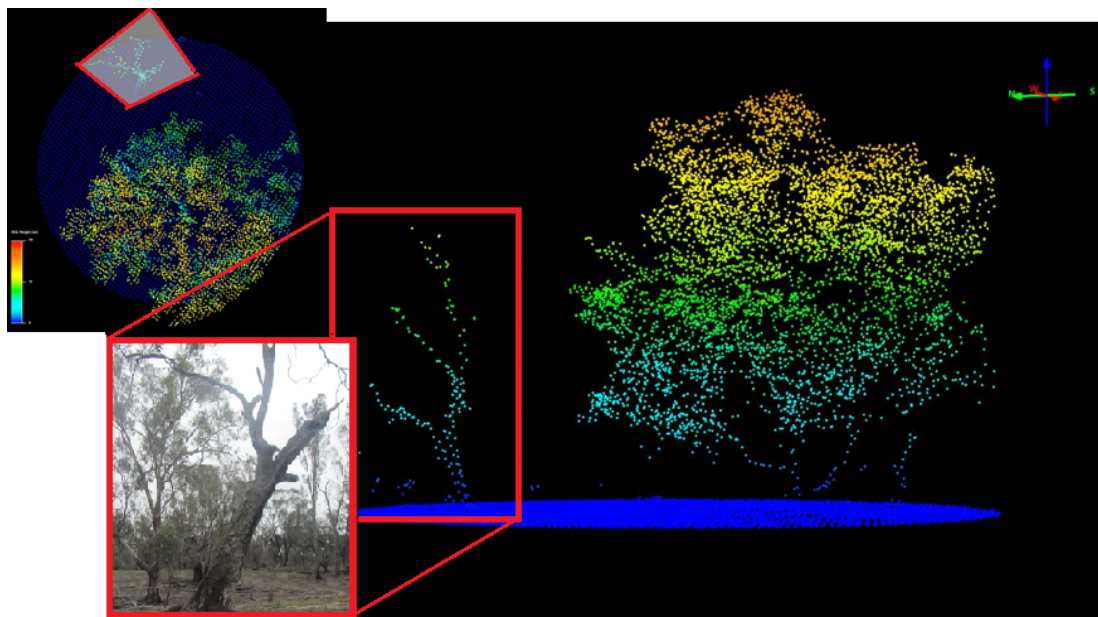


Figure 8-4: Example of a dead tree in relation to the discrete LiDAR point cloud.

8.3 Results

8.4 Discussion

Chapter 9

Comparison with Discrete Data

Furthermore, DASOS allows the user to choose whether the waveform samples or the discrete returns are inserted into the 3D density volume. Each sample or each return has a hit point and an intensity value. So, in both case the space is divided into 3D voxels and the intensity of each return or sample is inserted into the voxel it lies inside.

In general the results of discrete returns contain less information compared to the results from the FW LiDAR, even though the FW LiDAR contain information from about half of the emitted pulses (Section 3). As shown on the 1st example of table 3 the polygon mesh generated from the FW LiDAR contains more details comparing to the one created from the discrete LiDAR. The forest on the top is more detailed, the warehouses in the middle have a clearer shape and the fence on the right lower corner is continuous while in the discrete data it is disconnected and merged with the aliasing.

FW LiDAR polygons, compared to the discrete LiDAR ones, contain more geometry below the outlined surface of the trees. On the one hand this is positive because they include much information about the tree branches but on the other hand the complexity of the objects generated is high. A potential use of the polygon representations is in movie productions: instead of creating a 3D virtual city or forest from scratch, the area of interest can be scanned and then polygonised using our system.

But for efficiency purposes in both animation and rendering, polygonal objects should be closed and their faces should be connected. Hence, in movie productions, polygons generated from the FW LiDAR will require more post-processing in comparison with object generated from the discrete LiDAR.

Example 2 in table 3 shows the differences in the geometry complexity of the discrete and FW polygons using the x-ray shader of Meshlab. The brighter the surface appears the more geometry exists below the top surface. The brightness difference between area 1 and area 2 appears less in the discrete polygon.

Nevertheless, the trees in area 2 are much taller than in area 1, therefore more geometry should have existed in area 2 and sequentially be brighter. But the two areas are only well-distinguished in the FW LiDAR. On average the FW polygon is brighter than the discrete polygon, which implies higher geometry complexity in the FW polygon.

The comparison example 3 is rendered using the Radiance Scaling shader of Meshlab (Vergne et al, 2010). The shader highlights the details of the mesh, making the comparison easier. Not only the FW polygons are more detailed but also holes appear on the discrete polygons. The resolution of the voxels of those examples is 1.7m³ is, the bigger the holes are, while the full-waveform can be polygonised at a resolution of 1m³ without any significant holes. Figure 4 shows an example of rendering the same flightline of examples 3 at the resolution of 1m³ LiDAR data.

The last two examples (4 and 5) compare the side views of small regions. On the one hand the top of the trees are better-shaped in the discrete data. This may occur either because the discrete data contain information from double pulses than the FW data (Section 3) or because the noise threshold of the waveforms is not accurate and the top of the trees appear noisier on the FW LiDAR data. On the other hand more details appear close to the ground on the FW LiDAR data.

*** left during copying :s (and the higher the resolution, using FW)

Chapter 10

Overall Results

Chapter 11

Conclusions

11.1 Contributions

Bibliography

- [1] T. Elmqvist, C. Folke, M. Nyström, G. Peterson, J. Bengtsson, B. Walker, and J. Norberg, “Response diversity, ecosystem change, and resilience,” *Frontiers in Ecology and the Environment*, vol. 1, no. 9, pp. 488–494, 2003.
- [2] D. U. Hooper, F. S. Chapin Iii, J. J. Ewel, A. Hector, P. Inchausti, S. Lavorel, and B. Schmid, “Effects of biodiversity on ecosystem functioning: a consensus of current knowledge,” *Ecological monographs*, vol. 75, no. 1, pp. 3–35, 2005.
- [3] D. B. Lindenmayer and J. T. Wood, “Long-term patterns in the decay, collapse, and abundance of trees with hollows in the mountain ash (eucalyptus regnans) forests of victoria, southeastern australia,” *Canadian Journal of Forest Research*, vol. 40, no. 1, pp. 48–54, 2010.
- [4] R. L. Goldingay, “Characteristics of tree hollows used by australian birds and bats,” *Wildlife Research*, vol. 36, no. 5, pp. 394–409, 2009.
- [5] P. Gibbons and D. Lindenmayer, *Tree Hollows and Wildlife Conservation in Australia*. CSIRO Publishing, 2002.
- [6] “Animal pests: Poss.” <http://www.doc.govt.nz/conservation/threats-and-impacts/animal-pests/animal-pests-a-z/possums/>. Accessed: 19th of September 2014.
- [7] D. H. DeHayes, P. G. Schaberg, G. J. Hawley, and G. R. Strimbeck, “Acid rain impacts on calcium nutrition and forest health alteration of membrane-associated calcium leads to membrane destabilization and foliar injury in red spruce,” *Bio-Science*, vol. 49, no. 10, pp. 789–800, 1999.
- [8] J. Holmgren, “Prediction of tree height, basal area and stem volume in forest stands using airborne laser scanningce,” *Scandinavian Journal of Forest Research*, vol. 19, no. 6, pp. 543–553, 2004.

- [9] S. G. Aracil and R. B. A. Herries, D.L, “Evaluation of an additional lidar metric in forest inventory,” *Proceedings of Silvilaser*, 2015.
- [10] M. J. Harper, M. A. McCarthy, R. Van Der Ree, and J. C. Fox, “Overcoming bias in ground-based surveys of hollow-bearing trees using double-sampling,” *Forest Ecology and Management*, vol. 190, no. 2, pp. 291–300, 2004.
- [11] L. Rayner, M. Ellis, and J. E. Taylor, “Double sampling to assess the accuracy of ground-based surveys of tree hollows in eucalypt woodlands,” *Forest Ecology and Management*, vol. 36, no. 3, pp. 252–260, 2011.
- [12] R. B. Smith, *Introduction to Hyperspectral Imaging*. MicroImages, 2014.
- [13] W. Wanger, A. Ullrich, T. Melzer, C. Briese, and K. Kraus, “From single-pulse to ful-waveform airborne laser scanners,” *ISPRS Journal of Photogrammetry and Remote Sensing*, vol. 60, pp. 100–112, 2004.
- [14] A. Wehr and U. Lohr, “Airborne laser scanning - an introduction and overview,” *ISPRS Journal of Photogrammerty and Remote Sensing*, vol. 54, pp. 68–82, 1999.
- [15] C. Mallet and F. Bretar, “Full-waveform topographic lidar: State-of-the-art,” *ISPRS Journal of Photogrametry and Remote Sensing*, vol. 64, pp. 1–16, 2009.
- [16] K. Anderson, S. Hancock, M. Disney, and K. Gaston, “Is waveform worth it? a comparison of lidar approaches for vegetation and landscape characterization,” *Remote Sensing in Ecology and Conservation*, 2015.
- [17] A. Chauve, C. Mallet, F. Bretar, S. Durrieu, M. Deseilligny, and W. Puech, “Processing full-waveform lidar data: Modelling raw signals,” *International Archives of Photogrammetry, Remote Sensing and Spatial Information Sciences*, 2007.
- [18] *LAS Specification version 1.3-R1*. Bethesda, Maryland: American Society for Photogrammetry and Remote Sensing, 2010.
- [19] M. Warren, *Full Waveform Upgrade*. NERC ARSF wiki, 2012.
- [20] M. J. Sumnall, R. A. Hill, and S. A. Hinsley, “Comparison of small-footprint discrete return and full waveform airborne lidar data for estimating multiple forest variables,” *Remote Sensing of Environment*, vol. 173, pp. 214–223, 2016.
- [21] K. H. R. A. . Z. A. Lehner, H., “Consideration of laser pulse fluctuations and automatic gain control in radiometric calibration of airborne laser scanning data.,” *Proceedings of 6th ISPRS Student Consortium and WG VI/5 Summer School*, 2011.

- [22] I. Korpela, H. O. Ørka, H. V. Hyppä, J., and T. Tokola, “Range and agc normalization in airborne discrete-return lidar intensity data for forest canopies,” vol. 65, no. 4, pp. 369–379, 2010.
- [23] M. Isenburg, *LAStools - efficient tools for LiDAR processing*. rapidlasso.
- [24] M. Warren, B. Taylor, M. Grant, and J. D. Shutler, “Data processing of remorely sensed airborne hyperspectral data using the airborne processing library (apl),” *ScienceDirect, Computers and Geosciences*, vol. 64, 2014.
- [25] M. Isenburg, “Pulsewaves: An open, vendor-neutral, stand-alone, las-compatible full waveform lidar standard.,” 2012.
- [26] A. Persson, U. Soderman, J. Topel, and S. Ahlberg, *Visualisation and Analysis of full-waveform airborne laser scanner data*. V/3 Workshop, Laser scanning 2005, 2005.
- [27] M. Miltiadou, M. A. Warren, M. Grant, and M. Brown, “Alignment of hyperspectral imagery and full-waveform lidar data for visualisation and classification purposes,” *The International Archives of Photogrammetry, Remote Sensing and Spatial Information Sciences*, vol. 40, no. 7, p. 1257, 2015.
- [28] W. Wanger, A. Ullrich, V. Ducic, T. Maizer, and N. Studnicka, “Gaussian decompositions and calibration of a novel small-footprint full-waveform digitising airborne laser scanner,” *ISPRS Journal of Photogrammetry and Remote Sensing*, vol. 60, pp. 100–112, 2006.
- [29] A. Neuenschwander, L. Magruder, and M. Tyler, “Landcover classification of small-footprint full-waveform lidar data,” *Jounal of Applied Remote Sensing*, vol. 3, no. 1, pp. 033544–033544.
- [30] J. Reitberger, P. Krzystek, and U. Stilla, “Analysis of full waveform LiDAR data for tree species classification,” *International Journal of Remote Sensing*, vol. 29, no. 5, pp. 1407–1431, 2008.
- [31] A. Chauve, F. Bretar, S. Durrieu, M. Pierrot-Deseilligny, and W. Puech, “Fullanalyse: A research tool for handling, processing and analysing full-waveform lidar data,” *IEEE International Geoscience and Remote Sensing Symposium*, 2009.
- [32] P. Bunting, J. Armston, D. Clewley, and R. M. Lucas, “Sorted pulse data (spd) library—part ii: A processing framework for lidar data from pulsed laser systems in terrestrial environments,” *Computers & Geosciences*, vol. 56, pp. 207–215, 2013.

- [33] L. Cao, N. Coops, L. Innes, J. Dai, and H. Ruan, “Tree species classification in subtropical forests using small-footprint full-waveform lidar data,” *International Journal of Applied Earth Observation and Geoinformation*, vol. 49, pp. 39–51, 2016.
- [34] S. Hancock, K. Anderson, M. Disney, and K. J. Gaston, “Measurement of fine-spatial-resolution 3d vegetation structure with airborne waveform lidar: Calibration and validation with voxelised terrestrial lidar.,” *Remote Sensing of Environment*, vol. 188, pp. 37–50, 2017.
- [35] M. Miltiadou, M. Grant, M. Brown, M. Warren, and E. Carolan, “Reconstruction of a 3d polygon representation from full-wavefrom lidar data,” *RSPSoc Annual Conference 2014, New Sensors for a Changing World*, 2014.
- [36] R. Crippen, “Calculating the vegetation index faster,” *Remote Sensing of Environment*, vol. 34, no. 1, pp. 71–73, 1990.
- [37] R. N. Clark, G. A. Swayze, R. Wise, K. E. Livo, T. Hoefen, R. F. Kokaly, and S. J. Sutley, “Usgs digital spectral library splib06a,” *US Geological Survey, Digital Data Series*, vol. 231, 2007.
- [38] P. Hanrahan, “Ray tracing algebraic surfaces,” *ACM SIGGRAPH Computer Graphics*, vol. 17, no. 3., 1983.
- [39] H. Pfister, J. Harderbergh, J. Knittel, H. Lauer, and L. Seiler, “The volumepro real-time ray-casting system,” *Proceedings of the 26th annual conference on Computer graphics and interactive techniques*, pp. 251–260, 1999.
- [40] J. Nickolls, I. Buck, M. Garland, and K. Skadron, “Scalable parallel programming with cuda,” *Queue*, vol. 6, no. 2, pp. 40–55, 2008.
- [41] C. Crassin, F. Neyret, S. Lefebvre, and E. Eisemann, “Gigavoxels: Ray-guided streaming for efficient and detailed voxel rendering,” *Proceedings of the 2009 symposium on Interactive 3D graphics and games*, pp. 15–22, 2009.
- [42] J. F. Blinn, *A Generalization of Algebraic Surface Drawing*, vol. 1. ACM Transactions on Graphics (TOG).
- [43] A. Pasko and V. Savchenko, *Blending operations for the functionally based constructive geometry*. 1994.

- [44] W. E. Lorensen and H. E. Cline, “Marching cubes: A high resolution 3d surface construction algorithm,” *ACM Siggraph Computer Graphics*, vol. 21, pp. 163–169, 1987.
- [45] M. Levoy, “Volume rendering: Display of surfaces from volume data,” *IEEE Computer Graphics and Applications*, vol. 8, no. 3, pp. 29–37, 1998.
- [46] M. Hadwiger, J. Beyer, W. K. Jeong, and H. Pfister, “Interactive volume exploration of petascale microscopy data streams using visualization-driven virtual memory approach,” *IEEE Transactions on Visualization and Computer Graphics*, 2012.
- [47] S. Laine and T. Karras, “Efficient sparse voxel octrees,” *Visualization and Computer Graphics, IEEE Transactions*, vol. 17, no. 8, pp. 1048–1059, 2011.
- [48] B. Rodrigues de Araujo and J. A. Pires Jorge, *Adaptive polygonization of implicit surfaces*, vol. 29. Science Direct, Computer and Graphics, 2005.
- [49] E. Hartmann, “A marching method for the triangulation of surfaces,” *The Visual computer* 14, no. 14, no. 3, pp. 95–108, 1998.
- [50] C. D. Hansen and P. Hinken, “Massively parallel isosurface extraction,” *Proceedings of the 3rd conference on Visualization '92*, pp. 77–83, 1992.
- [51] C. Galbraith, P. MacMurchy, and B. Wyvill, *BlobTree Trees*. IEEE Computer Graphics International, 2004.
- [52] H. Sutter and A. Alexandrescu, *C++ Coding Standards: 101 Rules, Guidelines, and Best Practices*. United States: Addison-Wesley, 2004.
- [53] J. Wilhelms and A. Van Gelder, “Octrees for faster isosurface generation,” vol. 24, no. 5, 1990.
- [54] . W. J. Schaefer, S., “Dual marching cubes: Primal contouring of dual grids,” *Computer Graphics Forum*, vol. 24, no. 2, 2005.
- [55] J. Wilhelms and A. Van Gelder, “Octrees for faster isosurface generation,” *ACM Transactions on Graphics (TOG)*, vol. 11, no. 3, pp. 201–227, 1992.
- [56] S. F. Gibson, “Constrained elastic surface nets: Generating smooth surfaces from binary segmented data,” *International Conference on Medical Image Computing and Computer-Assisted Intervention*, pp. 888–898, 1998.
- [57] B. Chazelle and L. J. Guibas, “Fractional cascading: I. a data structuring technique.,” *Algorithmica*.

- [58] K. Museth, “Vdb: High-resolution sparse volumes with dynamic topology,” *ACM Transactions on Graphics (TOG)*, vol. 32, no. 3, p. 27, 2013.
- [59] M. S. Warren and J. K. Salmon, “A parallel hashed oct-tree n-body algorithm,” *In Proceedings of the 1993 ACM/IEEE conference on Supercomputing*, pp. 12–21, 1993.
- [60] M. Nießner, M. Zollhöfer, S. Izadi, and M. Stamminger, “Real-time 3d reconstruction at scale using voxel hashing,” *ACM Transactions on Graphics (TOG)*, vol. 32, no. 2, p. 169, 2013.
- [61] F. C. Crow, “Summed-area tables for texture mapping,” *ACM Computer Graphics*, vol. 18, no. 3, pp. 207–212, 1984.
- [62] S. Hanan, “Neighbor finding in images represented by octrees,” *Computer Vision, Graphics, and Image Processing*, vol. 46, no. 3, pp. 367–386, 1989.
- [63] G. Schrack, “Finding neighbors of equal size linear quadtrees and octrees in constant time,” *CVGIP: Image Understanding*, vol. 55, no. 3, pp. 221–230, 1992.
- [64] R. Lohner, “Robust, vectorized search algorithms for interpolation on unstructured grids,” *Journal of Computational Physics*, vol. 118, no. 2, pp. 380–387, 1995.
- [65] R. Castro, T. Lewiner, H. Lopes, G. Tavares, and A. Bordignon, “Statistical optimisation of octree searches,” *Computer Graphics Forum*, vol. 27, no. 6, pp. 1557–1566, 2008.
- [66] M. L. Clark, D. A. Roberts, J. J. Ewel, and D. B. Clark, “Estimation of tropical rain forest aboveground biomass with small-footprint lidar and hyperspectral sensors,” *ScienceDirect, Remote Sensing of Environment*, vol. 115.
- [67] J. E. Anderson, L. C. Plourde, M. E. Martin, B. H. Braswell, M. L. Smith, R. O. Dubayah, M. A. H. Dubayah, and J. B. Blair, “Integrating waveform lidar with hyperspectral imagery for inventory of a northern temperate forest,” *Remote Sensing of Environment*, vol. 112, no. 4, pp. 1856–1870, 2008.
- [68] H. Buddenbaum, S. Seeling, and J. Hill, “Fusion of full-waveform lidar and imaging spectroscopy remote sensing data for the characterization of forest stands,” *International Journal of Remote Sensing*, vol. 32, no. 13, pp. 4511–4524, 2013.
- [69] J. Heinzel and B. Koch, “Investigating multiple data sources for tree species classification in temperate forest and use for single tree delineation,” *International*

Journal of Applied Earth Observation and Geoinformation, vol. 18, pp. 101–110, 2012.

- [70] R. G. Congalton, “A review of assessing the accuracy of classifications of remotely sensed data,” *Remote Sensing of Environment*, vol. 37, no. 1.
- [71] J. F. Franklin, H. H. Shugart, and M. E. Harmon, “Tree death as an ecological process,” *BioScience*, vol. 17, no. 8, pp. 550–556, 1987.
- [72] J. Siitonen, “Forest management, coarse woody debris and saprophytic organisms: Fennoscandian boreal forests as an example,” *Ecological bulletins*, pp. 11–41, 2001.
- [73] I. Hanski, “Extinction debt and species credit in boreal forests: modelling the consequences of different approaches to biodiversity conservation,” *Annales Zoologici Fennici*, pp. 271–280, 2000.
- [74] G. Peterson, C. R. Allen, and C. S. Holling, “Ecological resilience, biodiversity, and scale.,” *Ecosystems*, vol. 1, no. 1, pp. 6–18, 1998.
- [75] N. Abrego and I. Salcedo, “How does fungal diversity change based on woody debris type? a case study in northern spain,” *Ekologija*, vol. 57, no. 3, 2011.
- [76] J. N. Stokland and K. H. Larsson, “Legacies from natural forest dynamics: Different effects of forest management on wood-inhabiting fungi in pine and spruce forests,” *Forest Ecology and Management*, vol. 261, no. 11, pp. 1707–1721, 2011.
- [77] D. Lonsdale, M. Pautasso, and O. Holdenrieder, “Wood-decaying fungi in the forest: conservation needs and management options,” *European Journal of Forest Research*, vol. 127, no. 1, pp. 1–22, 2008.
- [78] “List of extinct, threatened and near threatened australian birds,” *Environment Protection and Biodiversity Conservation Act*, 1999.
- [79] Government of Western Australia, “Oaks and wildlife the list of threatened and priority fauna list,” tech. rep., November 2015.
- [80] Y. Kim, Z. Yang, W. B. Cohen, D. Pflugmacher, C. L. Lauver, and J. L. Vankat, “Distinguishing between live and dead standing tree biomass on the north rim of grand canyon national park, usa using small-footprint lidar data.,” *Remote Sensing of Environment*, vol. 113, no. 11, pp. 2499–2510, 2009.
- [81] P. Polewski, W. Yao, M. Heurich, P. Krzystek, and U. Stilla, “Detection of fallen trees in als point clouds using a normalized cut approach trained by simulation,”

ISPRS Journal of Photogrammetry and Remote Sensing, vol. 105, pp. 252–271, 2015.

- [82] W. Mücke, B. Deák, H. M. Schroiff, A., and N. Pfeifer, “Detection of fallen trees in forested areas using small footprint airborne laser scanning data,” *Canadian Journal of Remote Sensing*, vol. 139, no. s1, pp. S32–S40, 2013.
- [83] W. Yao, P. Krzystek, and M. Heurich, “Identifying standing dead trees in forest areas based on 3d single tree detection from full-waveform lidar data,” *ISPRS Annals of the Photogrammetry, Remote Sensing and Spatial Information Sciences*, vol. I-7, pp. 359–364, 2012.
- [84] J. Pasher and D. J. King, “Mapping dead wood distribution in a temperate hard-wood forest using high resolution airborne imagery,” *Forest Ecology and Management*, vol. 258, no. 7, pp. 1536–1548, 2009.
- [85] I. Shendryk, M. Broich, M. G. Tulbure, A. McGrath, D. Keith, and S. V. Alexandrov, “Mapping individual tree health using full-waveform airborne laser scans and imaging spectroscopy: A case study for a floodplain eucalypt forest,” *Remote Sensing of Environment*, vol. 187, pp. 202–217, 2016.
- [86] S. C. Popescu, R. H. Wynne, and R. F. Nelson, “Measuring individual tree crown diameter with lidar and assessing its influence on estimating forest volume and biomass,” *Canadian journal of remote sensing*, vol. 29, no. 5, pp. 564–577, 2003.
- [87] L. Jing, B. Hu, J. Li, and T. Noland, “Automated delineation of individual tree crowns from lidar data by multi-scale analysis and segmentation,” 2012.
- [88] B. Hu, J. Li, L. Jing, and A. Judah, “Improving the efficiency and accuracy of individual tree crown delineation from high-density lidar data,” 2014.
- [89] S. C. Popescu and K. Zhao, “A voxel-based lidar method for estimating crown base height for deciduous and pine trees,” *Remote sensing of environment*, vol. 112, no. 3, pp. 767–781, 2008.
- [90] I. Shendryk, M. Broich, M. G. Tulbure, and S. V. Alexandrov, “Bottom-up delineation of individual trees from full-waveform airborne laser scans in a structurally complex eucalypt forest,” *Remote Sensing of Environment*, vol. 173, pp. 69–83, 2016.
- [91] J. L. Lovell, D. L. B. Jupp, G. J. Newnham, N. C. Coops, and D. S. Culvenor, “Simulation study for finding optimal lidar acquisition parameters for forest height retrieval.”

- [92] P. Viola and M. Jones, “Rapid object detection using a boosted cascade of simple features,” *Computer Vision and Pattern Recognition*, vol. 1, 2001.
- [93] P. Dong, “Characterization of individual tree crowns using three-dimensional space signatures derived from lidar data.,” *International Journal of Remote Sensing*, vol. 30, no. 24, pp. 6621–6628, 2009.
- [94] M. Sunnall, *Assessment of habitat condition and conservation status for lowland British woodland using earth observation techniques*. Bournemouth University: Unpublished PhD thesis, 2013.

Appendix A

DASOS user guide

Appendix B

Case Study: Field Work in New Forest

B.1 Introduction

This section is a case study containing field work from a non-professional perspective to better understand the challenges of working remotely with forests. Remotely sensed data contain a great amount of information but in order to build a good system for identifying trees and materials, an in depth knowledge of them is required [12]. For that reason, this case study was created; information about the New Forest, which is a forest in the south of United Kingdom, were collected and a small validation dataset was created. The dataset created includes the tree species and approximate heights of the trees in two areas of interest.

Before travelling to the New Forest, two areas of interest were selected. These areas were selected according to the following criteria:

- There were LiDAR data of the selected area to be able to compare what we can see in real life with the scanned data
- Areas that had a variation of tree species were selected. This was done according to the (non-validated) results of a thesis of Bournemouth University that classified the tree species of the New Forest [94]. This helped get a broader range of tree species.

The following sections give a detailed description of the information gathered during the trip. This includes the species and height maps generated, the different types of landscapes found and the challenges faced.

B.2 Validation Data Collected

The tree classes were initially defined by the provided Bournemouth thesis [94]. A colour was chosen for each tree class and, while being in the New Forest, the aim was to mark each tree on the paper map with the corresponding colour. Using QGIS (Quantum Geographic Information System) the classification results of the forest assessment, undertaken by Sumnall in 2013 [94], were coloured with the same colours to ease comparison.

At the aforementioned forest assessment, there were 26 classes from 14 different species; the remaining 12 classes were young versions of the 14 species. Here the classes are reduced to 14 by merging all the young trees into the tree species classes (in the 4 years gap between the 2010 assessment and the visit to new Forest in 2014, the young trees would have aged). See table B.1 for the initial 14 classes. Nevertheless, more tree species existed in the areas of interest in New Forest than those 14 classes. The colours and symbols of the extra tree classes are shown on table B.2.

Tree	Colour
1. Beech	Yellow
2. Oak	Orange
3. Silver Birch	Light Brown
4. Sweet Chestnut	Brown
5. Corsican Pine	Red
6. Coast Redwood	Pink
7. Douglas Fir	Purple
8. Grand Fir	Light Purple
9. Japanese Larch	Cyan
10. Lawson Cypress	Grey
11. Norway Spruce	Blue
12. Scots Pine	Green
13. Western Hemlock	Brown
14. Common Adler	Dark Brown

Table B.1: Colours of the initial 14 classes

During the visit, tree species maps were generated for a few square meters. The position of the trees were found relative to easily-spotted reference points (e.g. road crossing) that were marked in advance. That was done because, according to Dr. Ross Hill, no GPS can be accurate enough when trees are around since the satellite signal bounces off the leaves and reduces the positioning accuracy. In professional fieldwork, a total station is used but, for the purposes of this visit, it was not considered necessary. By the end of the case study, ground maps were coloured according to the tree species

Tree	Colour / Symbols
15. Ash	A
16. Hawthorn	Blue pen colour
17. <u>Malus (Crabapple)</u>	Highlighter
18. Holly Tree	
19. Trees that have been cut down	x
20. Trees that are mixed together	// (added on top of the normal colour)

Table B.2: Classes that were added during the trip

identified and estimates of the approximate heights of the trees were also noted down.

The following four maps were created for each selected area. The first two maps were created before the trip during preparation, while the last two contain the information collected during the field work.

- a screen shot of the area from Google map,
- the classification results from the forest assessment [94],
- the coloured tree species map and
- the approximated height map.

Comparing the validation dataset created with the classifications done at Bournemouth University (which were not validated), it is clear there are misclassifications. This is shown in Figures B-1 and B-2 and it is likely that occurs due to the over-segmentation of trees. Those wrong classifications justify that validation and field work data are essential for building a good classifier.

The first area is included in the LAS file named LDR-FW-FW10_01-201018715.LAS and it lies inside the limits: X = (433453 - 433761), Y = (102193 - 102405) [British National Grid coordinates]. The four maps that relate to these areas are shown in Figure B-1.

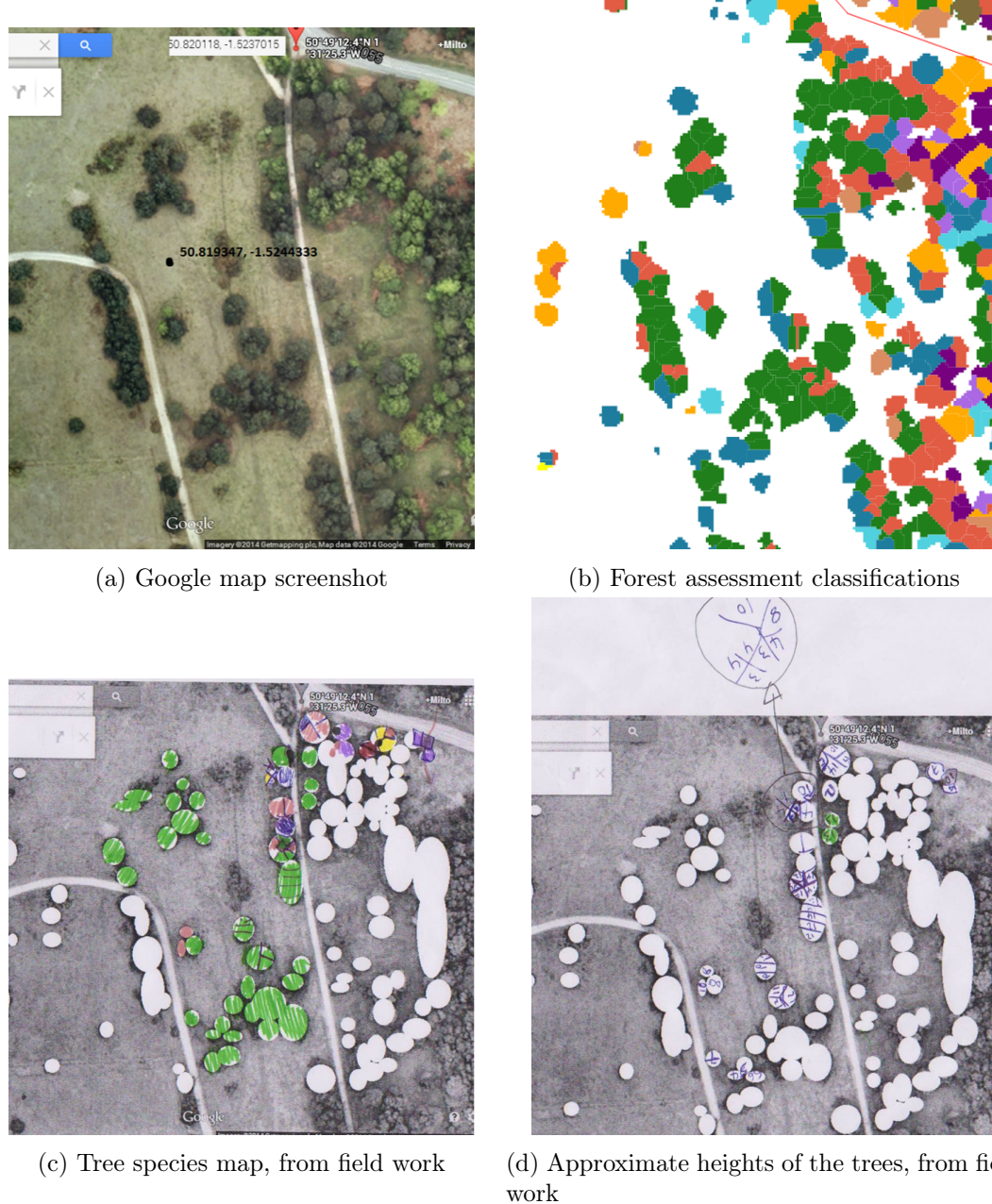
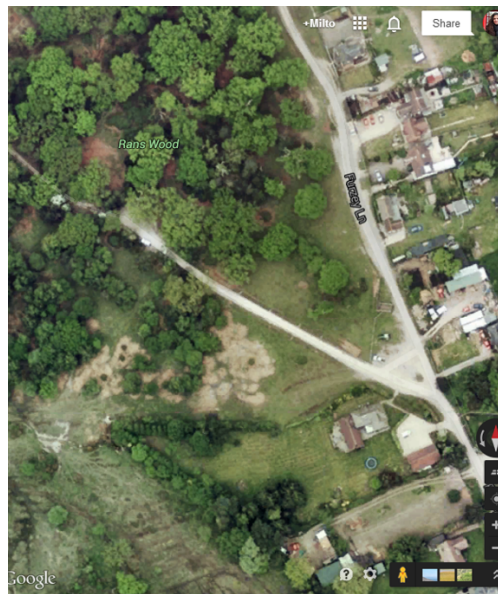
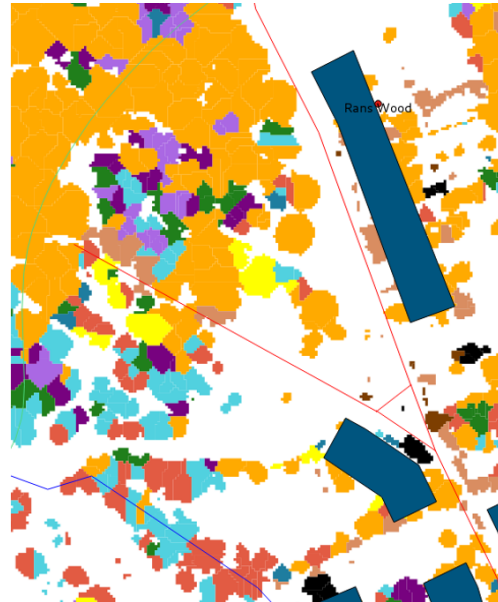


Figure B-1: The first area of interest and the related maps.

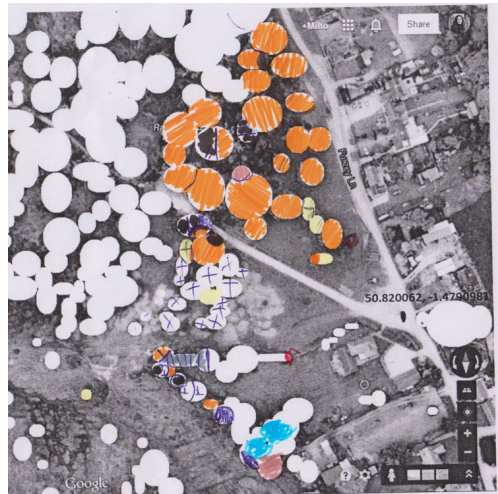
The second area is included in the LAS files named LDR-FW-FW10_01-201018719.LAS and LDR-FW-FW10_01-201018718.LAS and it lies inside the limits: X = (436442 - 436835), Y = (102334 - 102585) [British National Grid coordinates]. The four maps created for these areas are shown in Figure B-2.



(a) Google map screenshot



(b) Forest assessment classifications



(c) Tree species map, from field work



(d) Approximate heights of the trees, from field work

Figure B-2: The second area of interest and the related maps.

- > Wrong classification due to over segmentation of the trees.

B.3 Landscape types

During the forest assessment in New Forest, not only validation data were collected, but also useful information about classifying the data. The following images show examples of the five landscape types that were found in New Forest:

1. Heather fields:



Figure B-3: Trees that have been cut down

2. Grass with a few scattered trees:



Figure B-4: Grass with a few scattered trees

3. Dense Forest:



Figure B-5: Dense forest

4. Bushes and Shrubs



Figure B-6: Trees that have been cut down

5. Lakes and rivers, which are more rarely found



Figure B-7: Lakes and rivers

Please note that the landscape types could significantly differ according to the scanned area. For example, the landscape of New Forest is flat while the landscape of Eaves Wood (another scanned forest in UK) is hilly. The landscape type should be taken into consideration during classifications.

B.3.1 Classification challenges

This case study brought further understanding of the challenges of creating validation data and writing a tree species classifier. These challenges are listed and explained below with some photos taken during field work:

1. Field work and remotely sensed data collection should happen around the same time to avoid changes that happens over time. In the New Forest case, the airborne data were collected in 2010 and many changes occurred in the intervening time - in the most extreme cases, some trees had been cut down.
2. Machine learning becomes more challenging as the number of classes increases. Regarding tree species classes, it is unrealistic to expect that all tree species will be identified. This point is underlined by the fact that the list of tree species used in the



Figure B-8: Trees that have been cut down

tree assessment held by Sumnall [94] didn't include a number of trees (e.g. holly trees and crabapple) that were widespread in New Forest.

3. There is much more than just trees in the forest, including mobile animals, that may confuse a classification if LiDAR returns hit rocks, animals, vehicles or buildings instead of branches, leaves and trunks. Any classification must account for inevitable errors due to non-target objects being in the scene.



Figure B-9: Animals in New Forest

4. Large validation datasets from a single area will not be sufficient, because trees of the same species are usually gathered together. For instance, the first selected area has many pine trees while the second one has many oak trees. Therefore, it is important to have many field plots spread well within the area of interest.

5. Further, some trees are entwined together which makes it difficult to identify from the data whether they are one or two trees. Examples are shown in Figure B-10; in the left image, the trunks of the two trees are very close to each other and, in the right image, a crabapple and an oak tree have grown together.



Figure B-10: Trees, which are mixed together

B.4 Conclusions and Discussion

To sum up, the trip to the New Forest was essential for better understanding the challenges of remote monitoring of forests. During the visit, a small validation dataset was generated; the species and height of trees that are inside the two areas of interest were noted down. Field work is a time consuming task and weeks are required for generating a big enough validation dataset, but it is essential for understanding the object of interest (trees) in relation to the scanned data. Challenges identified were also explained and this increased knowledge about forests should lead to implementing a better classifier.